

Electronic, Magnetic and Mechanical Properties of Nd₂Fe₁₄B Permanent Magnets: Ab Initio Study

Baloyi M.E^{1*}, Ngoepe P.E¹ and Chauke H.R¹

Materials Modelling Centre, University of Limpopo, Private Bag X1106, 0727, Sovenga, South Africa

E-mail: mphamela.baloyi@gmail.com

Abstract. Neodymium-based permanent magnets (Nd₂Fe₁₄B) are the potential permanent magnets for use in various applications due to their high magnetic field strength and resistance to demagnetisation. These magnets have various applications in wind turbines and electric vehicles due to their exceptional magnetic properties. However, they suffer from low operating temperatures below 585 K. In this study, we investigate the electronic, magnetic, and mechanical properties of neodymium magnets using the first-principle density functional theory approach. Nd₂Fe₁₄B was found to be thermodynamically stable since the heats of formation were negative. However, it was found that Nd₂Fe₁₄B is mechanically unstable. Moreover, the density of states was calculated to predict the electronic stability of the permanent magnets which is in agreement with the calculated heats of formation. The phonon dispersion curves were also calculated and Nd₂Fe₁₄B is found to be vibrationally unstable due to the presence of soft modes. The calculated magnetic moment compares well to the experimental findings. The substitution of Nd with available rare earth elements is suggested to enhance the stability and magnetic properties of the magnets.

Keywords: Nd₂Fe₁₄B magnets, Permanent magnets, Density functional theory, Magnetic properties.

1. Introduction

Permanent magnet is a material that retains its magnetic properties because of its intrinsic structure [1]. PM includes a variety of magnets including alnico, ferrite, ceramic, and rare-earth magnets. They are used in a variety of applications including motors, generators, sensors, transducers, mechanical devices, latches, magnetic fields, and imaging systems [2]. Rare earth magnets (RE) are strong permanent magnets made from rare earth elements. However, REs are extremely brittle and very susceptible to corrosion; they are usually plated or coated to prevent corrosion [3].

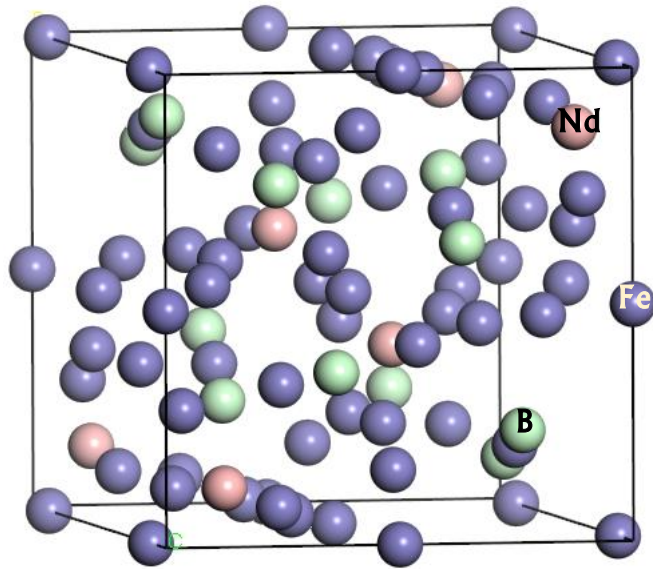
There are two types of well-known rare earth magnets namely samarium cobalt (SmCo₅) magnets and neodymium (NdFeB) magnets, with SmCo₅ magnets being less common due to their higher cost and lower magnetic field [4]. The strongest rare earth magnets are sintered NdFeB magnets, which have the highest energy product of any commercial PM material [5, 6]. These magnets are used in cutting-edge technological applications. In addition, experimental studies show that the highest magnetic properties were obtained at the highest milling time, suggesting that milling time increases the value of the magnetic properties. Small crystal sizes are required to obtain high magnetic properties in neodymium magnets [7]. Neodymium magnets have been reported to have high magnetic field strength and resistance to demagnetization. However, they suffer from extremely low operating temperatures, known as the Curie temperature (T_c) below 585 K [3]. In addition, the anisotropy field suffers a significant decrease with increasing temperature [8, 3].

In this work, we study the stability of Nd₂Fe₁₄B magnets using density functional theory (DFT)

techniques. Heats of formation, densities of states, elastic constants and phonon dispersion curves of $\text{Nd}_2\text{Fe}_{14}\text{B}$ structures were investigated. The calculations indicate that $\text{Nd}_2\text{Fe}_{14}\text{B}$ is vibrationally unstable. However, it was found that $\text{Nd}_2\text{Fe}_{14}\text{B}$ does not meet the tetragonal stability criteria, which is attributed to the mechanical instability of the material. In addition, the density of states was also calculated to predict the electronic stability of the permanent magnets.

2. Methodology

The calculations were carried out using *ab initio* density functional theory (DFT) [9] formalism as implemented in the Vienna *ab initio* simulation package (VASP) [10] with the projector augmented wave (PAW) [11]. An energy cut-off of 400 eV was used, as it was sufficient to converge the total energy of the tetragonal $\text{Nd}_2\text{Fe}_{14}\text{B}$ magnets. For the exchange-correlation functional, the generalized gradient approximation of Perdew, Burke and Ernzerhof (GGA-PBE)sol [12] was chosen. The suitable k-points mesh according to Monkhorst and Pack [13] of $6 \times 6 \times 3$ was used. A tetragonal $\text{Nd}_2\text{Fe}_{14}\text{B}$ structure with 68 atoms was used (Figure 1). The phonon dispersion spectra were evaluated using PHONON code [14] as implemented in MedeA software.



Atom	Site
Nd1	4g
Nd2	4f
Fe1	4e
F2	4c
Fe3	8j1
Fe4	8j2
Fe5	16k1
Fe6	16k2
B1	4g

Figure 1. The atomic arrangement unit cell of the $\text{Nd}_2\text{Fe}_{14}\text{B}$ system with a space group $P4_2/mmm$.

3. Results and discussion

3.1 Structural and Thermodynamic Properties

In Table 1, the lattice parameters and heats of formation for the tetragonal $\text{Nd}_2\text{Fe}_{14}\text{B}$ magnets are discussed. The magnet is a tetragonal structure consisting of a 68-atom unit cell and a space group of $P4_2/mmm$, with atoms arranged in an eight-layer structure, 56-Fe, 8-Nd and 4-B atoms. The calculated a parameter of $\text{Nd}_2\text{Fe}_{14}\text{B}$ was 8.249 Å whereas the c parameter was 12.12 Å. The results of the equilibrium lattice parameters agree with available experimental values ($a = 8.82$ Å and $c = 12.25$ Å) to within 6%. In addition, the heats of formation were calculated to determine the thermodynamic stability of the structure. The equation for determining the heats of formation (ΔH_f) is given by [23]:

$$\Delta H_f = E_c - \sum_i x_i E_i,$$

where E_c is the calculated total energy of the compound, E_i is the calculated total energy of element i in the compound. For a structure to be stable, the heat of formation must be negative; otherwise, a positive value indicates instability. Table 1 displays the heats of formation results for $\text{Nd}_2\text{Fe}_{14}\text{B}$ magnets. The heats of formation for the $\text{Nd}_2\text{Fe}_{14}\text{B}$ permanent magnet were found to be -6.499 eV/atom, indicating the

thermodynamic stability of the magnet.

Table 1. Lattice parameters and Heats of formation (ΔH_f) of the $\text{Nd}_2\text{Fe}_{14}\text{B}$ magnets.

Structure	Lattice parameter (Å)		ΔH_f (eV/atoms)
	Calculated	Experimental [3]	
$\text{Nd}_2\text{Fe}_{14}\text{B}$	$a = 8.25$	$a = 8.82$	-6.499
	$b = 8.25$	$b = 8.82$	
	$c = 12.12$	$c = 12.25$	

3.2. Density of states

To further understand the difference in electronic structures of the $\text{Nd}_2\text{Fe}_{14}\text{B}$ magnets, the partial density of states (DOS) are determined and the plots are shown in Figure 2 below. The partial density of states (PDOS) was calculated to determine the contribution of Nd, Fe, and B atomic orbitals. We note that the lower energy side is dominated by sets of peaks originating primarily from the d states of Fe, p states, and s states of B. On the lower energy side, the Fe 3d orbitals dominate from the Fermi level (0 eV) to -6 eV, while the B s-orbital is responsible for the peaks at -8 eV and -9 eV. The peaks of Fe 3d-states are clustered from -5 eV to 1 eV whereas B peaks around -5 eV to 0 eV, -8 eV and -9 eV. The highly localized Nd peaks are found to be located clustered around the E_f as shown in Figure 2. The f states of Nd are responsible for the higher energy peaks. We observe that f states of Nd and d states of Fe contribute to the observed peaks in the conduction band, with f states of Nd dominating. Boron does not influence the conduction band. Both Fe d-orbitals and Nd f-orbitals are responsible for the peaks at the E_f . The s and p orbitals of both Nd and Fe contribute less to the E_f peaks. The total DOS for $\text{Nd}_2\text{Fe}_{14}\text{B}$ is dominated by the Fe 3d states as shown in Figure 2. In the E_f , the extremely localized peaks are observed to be clustered. Moreover, the E_f hits the DOS at the pseudogap which suggests that the structure is stable. As has been seen in the heats of formation, our total density of states calculations confirms that the $\text{Nd}_2\text{Fe}_{14}\text{B}$ structure is electronically stable. This study compares to a previous report on the tDOS of $\text{Nd}_2\text{Fe}_{14}\text{B}$ [15].

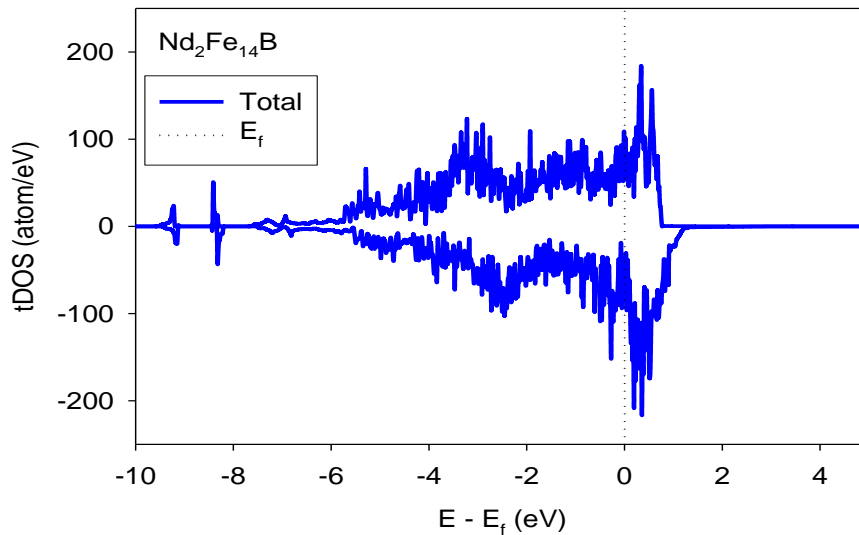


Figure 2. The total density of states for the $\text{Nd}_2\text{Fe}_{14}\text{B}$ permanent magnets.

Figure 3. The partial density of states for the Nd₂Fe₁₄B permanent magnets.

3.3. Elastic Constants

The elastic constants, bulk, shear, Young moduli, Pugh, Poisson, and anisotropic ratios of Nd₂Fe₁₄B magnets are listed in Table 2. The following is the condition of tetragonal crystal stability [16]:

$$C_{44} > 0, C_{66} > 0, C_{11} > |C_{12}| \text{ and } C_{11} + C_{12} - \frac{2C_{13}^2}{C_{33}} > 0. \quad (1)$$

The C_{11} is found to be greater than the absolute of C_{12} whereas the C_{44} and C_{66} are greater than zero. Moreover, two elastic constants are negative, namely C_{13} and C_{33} with values of -1412.67 and -2594.39, respectively. The calculated elastic shear modulus was found to be positive ($C' = 110.96$). This suggests that the computed elastic constants of Nd₂Fe₁₄B satisfy tetragonal mechanical stability criteria (eq. 1). To deduce the mechanical strength of materials the elastic anisotropy (A) factor is used [17]. If the value of A is 1, the material is considered to be elastically isotropic (fewer microcracks within the material) and the degree of anisotropy is measured if the material is less than or greater than 1 [18]. Elastic anisotropy for non-cubic is

indicated by A_1 , A_2 and A_3 . The calculated A_1 , A_2 and A_3 of $\text{Nd}_2\text{Fe}_{14}\text{B}$ magnets all show anisotropic behaviour with values of 0.56, 0.31 and 1.79, respectively.

In addition, we calculated the bulk to shear modulus (B/G) ratio, known as Pugh's ratio to investigate the fracture range or the ductility in these structures. Pugh proposed that material is ductile if Pugh's ratio is greater than 1.75 ($B/G > 1.75$) otherwise brittle [19]. It is found that the B/G of the $\text{Nd}_2\text{Fe}_{14}\text{B}$ phase is -14.42, which is smaller than 1.75, so $\text{Nd}_2\text{Fe}_{14}\text{B}$ is a brittle phase. The magnetic moment of the $\text{Nd}_2\text{Fe}_{14}\text{B}$ structure was calculated as shown in Table 2 below. The calculated magnetic moment was 35.63 B, which agrees well with the experimental values of 35.0 B/f.u or 37.1 B/f.u [20, 3].

Table 2. Elastic constants, anisotropy, Pugh's ratio and magnetic moment of $\text{Nd}_2\text{Fe}_{14}\text{B}$ permanent magnets.

Properties	Calculated
C_{11}	472.47
C_{12}	250.56
C_{13}	-1412.67
C_{16}	449.37
C_{33}	-2594.39
C_{44}	110.36
C_{66}	61.82
C'	110.96
$A_1 = 2C_{66}/(C_{11}-C_{12})$	0.56
$A_2 = 2C_{66}/(C_{11}-C_{12})$	0.31
$A_3 = 2C_{44}/(C_{11} + C_{33} - 2C_{13})$	1.79
B/G	-14.42
Magnetic Moment	35.63

3.4. Phonon dispersions curves

Phonon dispersion curves and phonon density of states (DOS) for the $\text{Nd}_2\text{Fe}_{14}\text{B}$ magnets are presented in Figure 4. The phonon dispersion is used to investigate the vibrational stability of these magnets, where the presence of soft modes in the negative frequency suggests the instability of the material otherwise stability. As it has been seen in the elastic properties, our phonon dispersion calculations (Figure 4) confirm that the $\text{Nd}_2\text{Fe}_{14}\text{B}$ structure is vibrational unstable since there are soft modes observed in the phonon calculations. The soft modes are observed along X, M, Z, A, R and Γ directions. There are vibrations observed at -27 THz in the negative frequency along the Γ directions which indicate the instability of the material.

There is a small sharp peak along -7 THz which indicates the contribution of Nd, which is also ascribed to the DOS peak at 0 THz and 10 THz. Moreover, Fe is ascribed to the DOS peak around 15 THz and it is also responsible for vibrations in the negative frequency. B atom has a negligible effect or contribution towards the negative frequency, however, it is ascribed to the DOS peak at 18 THz. This suggests that Nd and Fe vibrations are responsible for the instability of the $\text{Nd}_2\text{Fe}_{14}\text{B}$ structure.

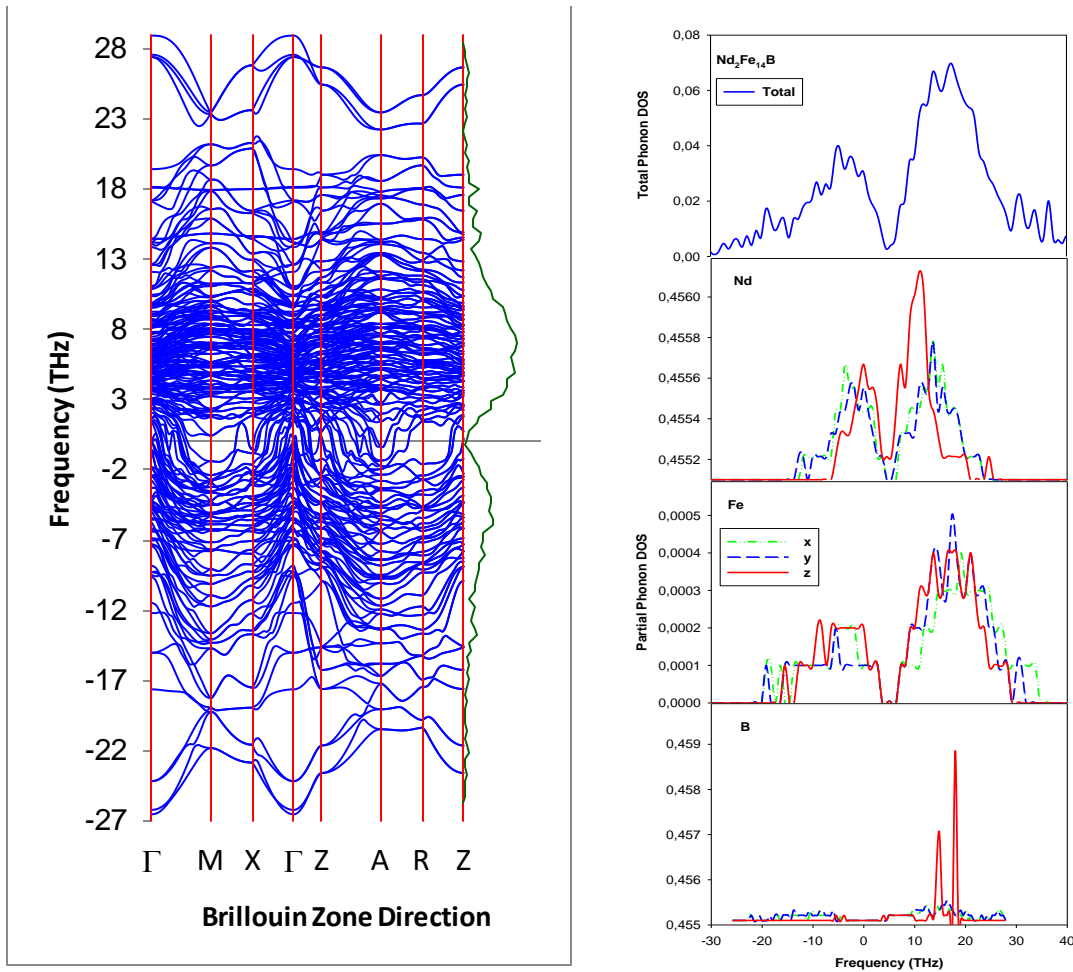


Figure 4. Phonon dispersions and phonon density of states for $\text{Nd}_2\text{Fe}_{14}\text{B}$ permanent magnets.

4. Conclusions

The equilibrium lattice parameter, heats of formation, elastic properties, vibrational properties and electronic properties of $\text{Nd}_2\text{Fe}_{14}\text{B}$ magnets were calculated using ab initio. It was found that the lattice parameter for $\text{Nd}_2\text{Fe}_{14}\text{B}$ structures is in good agreement with the experimental findings. $\text{Nd}_2\text{Fe}_{14}\text{B}$ is found to be thermodynamically stable with negative heats of formation, which is in good agreement with the calculated density of states. In addition, all of the elastic constants satisfy tetragonal stability criteria. The phonon dispersion curves show that the neodymium system is vibrationally unstable due to soft modes observed in the negative frequency. In conclusion, $\text{Nd}_2\text{Fe}_{14}\text{B}$ magnets are found to be unstable and the partial substitution of Nd with RE is suggested to enhance the stability and magnetic properties of magnets.

Acknowledgements

The authors would like to thank the National Research Foundation (NRF) for its financial support. The Department of Science and Innovation (DSI) is widely acknowledged. The calculations were carried out on computers at the University of Limpopo's Materials Modelling Centre (MMC) and the Centre for High-Performance Computing (CHPC) in Cape Town.

References

- [1] J. M. D. Coey. *Scripta Materialia*, **67**, 524-529, (2012)
- [2] Q. Gong, M. Yi, R. F. L. Evans, O. Gutflisch and B. Xu. *Materials Research Letters*, **8**, 89-96, (2020)

- [3] M. Sagawa, S. Fujimura, H. Yamamoto and Y. Matsuura. *IEEE Transactions on Magnetics*, **20**, 1584-1589, (1984)
- [4] X. Yin, M. Yue, Q. Lu, F. Wang, Y. Qiu, W. Liu, T. Zuo, S. Zha, X. Li and X. Yi. *Eng.* **6**, 165-172, (2020)
- [5] J. M. D. Coey. *IEEE Transactions on Magnetics*, **47**, 4671-4681, (2011)
- [6] J. Yang, J. Han, H. Tian, L. Zha, X. Zhang, C. S. Kim, D. Liang, W. Yang, S. Liu and C. Wang. *Eng.* **6**, 132-140, (2020)
- [7] Ramlan, Muljadi, P. Sardjono, F. Gulo and D. Setiabudidaya. *J. Physics: Conf. Series*, **776**, 1-6, (2016)
- [8] Q. Tian, L. Zha, w. Yang and Q. Qiao. *AIP advances*, **8**, 1-6, (2018)
- [9] W. Kohn and L. J. Sham. *Pack. Phys. Rev. B*, **140**, 1133-1138, (1965)
- [10] G. Kresse and J. Hafner *Pack. Phys. Rev. B*, **49**, 251-269, (1994)
- [11] G. Kresse and D. Joubert. *Pack. Phys. Rev. B*, **59**, 1758-1775, (1999)
- [12] P. Perdew, K. Burke and M. Enzerhof. *Phys. Rev. Lett.*, **77**, 3865-3868, (1996)
- [13] H. J. Monkhorst and J. D. Pack. *Phys. Rev. B*, **13**, 5188-5192, (1976)
- [14] K. Parlinski, Z. Q. Li and Y. Kawazoe. *Phys. Rev. Lett.*, **78**, 4063-4066, (1997)
- [15] A. E. Aly. *International Journal of Pure and Applied Physics*, **5**, 215-229, (2009)
- [16] M. J. Phasha, P. E. Ngoepe, H. R. Chauke, D. G. Pettifor and D. Nguyen-Mann. *Intermetallics*, **18**, 2083-2089, (2010)
- [17] A. Sekkal, M. Sahlaoui and A. Benzair. *Intermetallic Compounds*, **73189**, 193-202, (2018)
- [18] R. Mahlangu, H. R. Chauke, P. E. Ngoepe and M. J. Phasha. *Intermetallics*, **33**, 27-32, (2013)
- [19] S. F. Pugh. *J. Sci.*, **45**, 823-843, (1954)
- [20] E. Burzo. *Reports on Progress in Physics*, **61**, 1099-1105, (1998)
- [21] G. V. Sin'ko and N. A. Smirnov. *J. Physics: Condensed Matter*, **14**, 6989-7005, (2002)
- [22] R. G. Hennig, A. E. Carlsson, K. F. Kelton and C. L. Henley. *Phys. Rev. B*, **71**, 144103, (2005)
- [23] V. Tvergaard, and J. W. Hutchinson. *J. Am. Ceram. Soc.*, **71**, 157-163, (1988)
- [24] H. Fu, D. Li, F. Peng, T. Gao, and X. Cheng. *Comput. Mater. Sci.*, **44**, 774-778, (2008)